Analytic model for electrostatic fields in surface-electrode ion traps

M. G. House*
Department of Physics and Astronomy, University of California–Los Angeles, Los Angeles, California 90095, USA
(Received 26 May 2008; published 2 September 2008)

The design of surface-electrode ion traps is studied analytically. The classical motion of a single ion in such a trap is described by coupled Mathieu equations. An analytic boundary-value solution for the Laplace equation in three dimensions with a piecewise-constant Dirichlet boundary condition is described. This solution is used to model the electrostatic potential field generated by a series of electrodes lying in a single plane. The model is applied to the problem of designing surface-electrode ion traps, including calculating important trap design parameters such as the center position of the trapped ion, trap depth, and stability parameters. The model is used to determine optimized dimensions for trap electrodes in various cases.

DOI: 10.1103/PhysRevA.78.033402 PACS number(s): 37.10.Gh, 37.10.Ty, 41.20.Cv

I. INTRODUCTION

The linear Paul trap has been used for many years to trap, store, and control ions [1,2]. In such a trap ions are typically confined in two dimensions by electric fields oscillating at radio frequency (rf), and in the third dimension by a static electric potential well. A recent design development has been to construct the trap out of electrodes mounted on a flat surface [3]. The "surface-electrode" design may be favorable because the trap can be constructed using photolithographic fabrication techniques, which allow construction of complex traps and small electrode dimensions. It is hoped that small, complex structures will be a means of scaling up quantum information processing to a large number of qubit operations using trapped ions [4–6]. Several traps employing this type of design have now been demonstrated [7–12]. Surface-electrode traps also have the advantage of increased optical access compared to traditional Paul traps. The chief disadvantage of the surface-electrode design is the relatively small potential well that confines the ions, limiting the energy at which they can be trapped. Since techniques for loading ions into a surface trap and cooling them have been demonstrated, this weakness does not seem to be fatal.

To date surface-electrode ion trap experiments have relied primarily on numerical simulations of electrostatic fields in designing the geometry of the trap electrodes to achieve desired fields. The purpose of this article is to describe an analytical model for the electrostatic fields of a surface-electrode trap and to use it to provide insight into trap design. The analytic model provides a faster and more precise means to compute the electrostatic fields, as well as the opportunity to determine and analyze trap design characteristics more directly. Closed-form expressions for some of the important trap parameters are developed here and used to determine optimized trap dimensions.

Previous types of Paul trap have had sufficient symmetry that the three-dimensional equations of motion of an ion in the trap could be decomposed into three one-dimensional equations. Because of the reduced symmetry in surface electrode ion traps compared to more traditional Paul traps, the equations of motion of an ion in the trap cannot be decoupled in general. In Sec. II we develop the theory of the classical equations of motion of a single trapped ion in a three-dimensional Paul trap potential and analyze them using multidimensional Floquet theory. The coupling of the equations of motion makes a description of the motion more complex, but does not fundamentally change the nature of the motion. As in the one-dimensional case, the motion is characterized by a relatively low frequency "secular" oscillation superimposed on high frequency "micromotion" oscillations.

The model used to describe the electrostatic fields in the trap is introduced in Sec. III. The electric potential is determined by solution of the Laplace equation with Dirichlet boundary conditions. In Secs. IV and V the model is applied to the problem of determining the working parameters of an ion trap and determining optimal geometries for the trap electrodes.

The coordinate convention used in this article is: $x=x_1$ is the direction parallel to the electrode surface and perpendicular to the axial dimension of the trap. $y=x_2$ is the direction normal to the electrode surface. $z=x_3$ is the axial dimension of the trap.

II. ION MOTION

A Paul trap in general uses a combination of a static potential ϕ_{dc} and a potential ϕ_{rf} oscillating at angular frequency Ω to confine the motion of an ion so that the total field is

$$\phi(x,y,z,t) = \phi_{\mathrm{dc}}(x,y,z) + \phi_{\mathrm{rf}}(x,y,z)\cos(\Omega t). \tag{1}$$

At the point where a charged particle is to be trapped, the gradient of both parts of the potential will be zero. The potential expanded to second order in the coordinates is

$$\phi(x,y,z,t) = \frac{1}{2}\sum_{i,j}\left(\frac{\partial^2\phi_{\mathrm{dc}}}{\partial x_i \partial x_j}\right)x_i x_j + \frac{1}{2}\cos(\Omega t)\sum_{i,j}\left(\frac{\partial^2\phi_{\mathrm{rf}}}{\partial x_i \partial x_j}\right)x_i x_j, \tag{2}$$

where x_i are the displacements of the ion from the trap center in each dimension and the derivatives are evaluated at the trap center. The classical equations of motion for a particle of mass m and net charge Ze in such a field are

*house@physics.ucla.edu

 ©2008 The American Physical Society

$$m\frac{d^2x_i}{dt^2} = -Ze\sum_j \left[\left(\frac{\partial^2\phi_{\mathrm{dc}}}{\partial x_i \partial x_j}\right) + \left(\frac{\partial^2\phi_{\mathrm{rf}}}{\partial x_i \partial x_j}\right)\cos(\Omega t)\right] x_j. \quad (3)$$

This can be rewritten in the canonical form of the vector Mathieu equation

$$\frac{d^2\boldsymbol{x}}{d\tau^2} + [A + 2Q\cos(2\tau)]\boldsymbol{x} = 0, \quad (4)$$

where $\tau = \Omega t/2$ is a scaled time parameter and the elements of the matrices A and Q are

$$A_{ij} = \frac{4Ze}{m\Omega^2}\left(\frac{\partial^2\phi_{\mathrm{dc}}}{\partial x_i \partial x_j}\right), \quad Q_{ij} = \frac{2Ze}{m\Omega^2}\left(\frac{\partial^2\phi_{\mathrm{rf}}}{\partial x_i \partial x_j}\right). \quad (5)$$

In some literature A is called the stiffness matrix and Q the excitation matrix. They are the multidimensional generalizations of the stability parameters a and q commonly described in ion trap literature. A and Q are symmetric and are required by the Laplace equation to have zero trace. If they are diagonal, the matrix equation can be directly separated into three independent one-dimensional Mathieu equations. More generally, if A and Q commute, a coordinate basis can be found in which both matrices are simultaneously diagonal and the equations similarly separate [13]. In some cases where A and Q do not commute it may still be possible to separate one coordinate equation from the other two. In most types of Paul trap, the equations have been separable (or assumed to be so) and the one-dimensional Mathieu equation has been widely discussed in ion trap literature [2,5,14]. The directions of the independent modes (the simultaneous eigenvectors of A and Q) are usually called the principal axes of the trap, but this definition loses meaning when the equations are coupled.

If the ion equations of motion are not separable, they may be analyzed by application of multidimensional Floquet theory [15,16]. Equation (4) can be restated as a first-order differential equation

$$\dot{\boldsymbol{u}} = F(\tau)\boldsymbol{u}, \quad (6)$$

by defining the block matrices

$$\boldsymbol{u} = \begin{pmatrix} \boldsymbol{x} \\ \dot{\boldsymbol{x}} \end{pmatrix}, \quad F(\tau) = \begin{pmatrix} 0 & I \\ A + 2Q\cos(2\tau) & 0 \end{pmatrix}, \quad (7)$$

where I is the 3×3 identity matrix, 0 is the 3×3 zero matrix, and dots represent differentiation with respect to τ. Because $F(\tau)$ is periodic, $F(\tau+\pi)=F(\tau)$, this equation has independent solutions $\boldsymbol{u}_i(\tau)$ of the form

$$\boldsymbol{u}_i(\tau) = \exp(\mu_i\tau)\boldsymbol{b}_i(\tau), \quad (8)$$

where $\boldsymbol{b}_i(\tau)$ is periodic with period π. To determine the characteristic exponents μ_i, integrate (numerically) the matrix differential equation

$$\dot{U}(\tau) = F(\tau)U(\tau) \quad (9)$$

beginning with $U(0)=I$ to determine $U(\pi)$. Taking the eigenvalues λ_i of $U(\pi)$, the characteristic exponents are $\mu_i = \ln(\lambda_i)/\pi$. From the definition of F it can be seen that F is a Hamiltonian matrix which obeys $KF+F^TK=0$, where K is the skew-symmetric matrix

$$K = \begin{pmatrix} 0 & -I \\ I & 0 \end{pmatrix}. \quad (10)$$

Using this property it can be shown that if Eq. (8) is a solution of Eq. (6), then there is another solution of the same form with $\mu_j=-\mu_i$, $\boldsymbol{b}_j=K\boldsymbol{b}_i$; thus the characteristic exponents always appear in opposite pairs. If the real part of any characteristic exponent is nonzero, then either it or its opposite pair represents a mode in which the motion grows exponentially in time; the motion is unstable. If the real part of μ_i is zero for all i, the ion motion will be stable and the factor $\exp(\mu_i\tau)=\exp(i\beta_i\tau)$ will describe a sinusoidal oscillation at frequency $\omega_i=\beta_i\Omega/2$. This oscillation is called the secular motion of the ion and ω_i the secular frequency. Calculation of the characteristic exponents is important in order to verify that the ion motion is stable for a particular electric field configuration, and to determine the secular frequencies.

The solution (8) can be further analyzed by expanding $\boldsymbol{b}(\tau)$ in a Fourier series (leaving off the subscript i)

$$\boldsymbol{u}(\tau) = \exp(\mu\tau)\sum_{n=-\infty}^{\infty}\boldsymbol{b}_n e^{2in\tau}. \quad (11)$$

For a stable motion, $\boldsymbol{b}_0$ represents the amplitude and direction of the lowest frequency motion of the ion in the trap, the secular motion. The higher order components of the expansion represent higher frequency oscillations that are known as the micromotion. The vector $\boldsymbol{b}_0$ is the direction along which the secular motion occurs for an individual mode; it is the most interesting component because the secular motion is generally the largest amplitude and it is the secular motion that is interacted with experimentally, for example when Doppler cooling the ion. In the case of coupled Mathieu equations the micromotion for a particular mode may not be in the same direction as the secular motion.

Substituting Eq. (11) into the equation of motion (4) yields the constraint

$$(A + Qe^{2i\tau} + Qe^{-2i\tau})e^{\mu\tau}\sum_{n=-\infty}^{\infty}\boldsymbol{b}_n e^{2in\tau} + e^{\mu\tau}\sum_{n=-\infty}^{\infty}(2in+\mu)^2\boldsymbol{b}_n e^{2in\tau} = \boldsymbol{0}. \quad (12)$$

In this equation each set of terms with of equal factors of $e^{2in\tau}$ must individually sum to zero, which leads to the recursive relationship

$$(2in+\mu)^2\boldsymbol{b}_n + A\boldsymbol{b}_n + Q\boldsymbol{b}_{n-1} + Q\boldsymbol{b}_{n+1} = \boldsymbol{0} \quad (13)$$

between the Fourier coefficients $\boldsymbol{b}_n$. By substituting this equation into itself repeatedly we can arrive at the forms

$$\boldsymbol{b}_n = \{G_n - [G_{n+1} - (G_{n+2} - \ldots)^{-1}]^{-1}\}^{-1}\boldsymbol{b}_{n-1}, \quad n > 0,$$

$$\boldsymbol{b}_n = \{G_n - [G_{n-1} - (G_{n-2} - \ldots)^{-1}]^{-1}\}^{-1}\boldsymbol{b}_{n+1}, \quad n < 0, \tag{14}$$

where $G_n = -Q^{-1}[(2in+\mu)^2 I + A]$. From Eq. (14) all of the amplitudes $\boldsymbol{b}_n$ can be determined in terms of $\boldsymbol{b}_0$. Combining Eq. (13) with $n=0$ and Eq. (14), $\boldsymbol{b}_0$ is determined up to a scalar amplitude by the homogeneous equation

$$\{[\mu^2 I + A] + Q[G_1 - (G_2 - \cdots)^{-1}]^{-1} + Q[G_{-1} - (G_{-2} - \cdots)^{-1}]^{-1}\}\boldsymbol{b}_0 = \mathbf{0}. \tag{15}$$

The infinite sequence of matrices in these expressions can generally be truncated after only a few terms because they quickly become small with increasing $|n|$. In the complex domain there are six amplitudes that determine the motion, corresponding to an amplitude and phase of each of three independent modes of motion in the real domain. It may be worth noting that, in cases studied, when the motion is stable the secular motion directions $\boldsymbol{b}_0$ are approximately in the same directions as the eigenvectors of A, which indicates that it is primarily the shape of the dc potential field that determines the directions of secular motion, not the rf potential.

In the limit that $|\boldsymbol{b}_0| \gg |\boldsymbol{b}_{\pm 1}| \gg |\boldsymbol{b}_{\pm 2}|$, which is true when $\beta \ll 1$, the secular motion of the ion can be characterized approximately in terms of a pseudopotential energy [17]

$$\psi(x,y,z) = \frac{Z^2 e^2}{4m\Omega^2}|\nabla \phi_{\mathrm{rf}}|^2. \tag{16}$$

This pseudopotential represents the kinetic energy of the micromotion of the particle, which can be interpreted as a potential energy when examining only the secular motion of the ion. The pseudopotential approximation is our best tool for characterizing the maximum energy at which an ion can be contained in the trap.

III. ELECTROSTATIC POTENTIAL MODEL

The electric fields used to confine ions as described in the previous section must be generated by an experimental aparatus. Here we assume that the electrostatic field is created by a set of conducting electrodes whose upper surfaces are in the plane $y=0$. The layout of individual electrodes in the plane and the voltages applied to them are chosen by the experimenter in order to create a desirable field.

The electrostatic potential $\phi(x,y,z)$ in a charge free region above the electrodes obeys the Laplace equation

$$\nabla^2 \phi = 0. \tag{17}$$

If the electrodes are collectively assumed to occupy the entire $y=0$ plane, extending infinitely in the x and z dimensions and with infinitely small gaps between them (see the Appendix), then the voltages applied to the individual electrodes define the potential $\phi(x,0,z)$. On each electrode the potential is constant, so $\phi(x,0,z)$ is piecewise constant. The problem of finding ϕ in the space $y>0$ can be stated as a boundary-value problem [18]. In addition to the requirement that ϕ be equal to the voltages applied to the electrodes on $y=0$, in this model it is also restricted so that the potential drops to zero as $y \to \infty$, and that it be finite as $x \to \pm\infty$ and $z \to \pm\infty$. The general form of the solution given these boundary conditions is

$$\begin{aligned}\phi(x,y,z) = \int_0^\infty dk_z \int_0^\infty dk_x e^{-\sqrt{k_x^2+k_z^2}y}[&A_1(k_x,k_z)\cos(k_x x)\cos(k_z z) \\ &+ A_2(k_x,k_z)\sin(k_x x)\cos(k_z z) \\ &+ A_3(k_x,k_z)\cos(k_x x)\sin(k_z z) \\ &+ A_4(k_x,k_z)\sin(k_x x)\sin(k_z z)].\end{aligned} \tag{18}$$

Here the values A_i are degrees of freedom in the general solution of the differential equation that must be determined in order to satisfy the boundary condition $\phi(x,0,z)$ for a specific electrode geometry and applied voltages. In this case they collectively represent the two-dimensional Fourier transform of $\phi(x,0,z)$. The field $\phi(x,y,z)$ created by a set of electrodes can be constructed by finding the field of the electrodes individually and summing them together, so we can first examine the field of a single electrode. Consider a rectangular electrode with opposite corners at positions $(x_1,0,z_1)$ and $(x_2,0,z_2)$, held at voltage V in an otherwise grounded electrode plane

$$\phi(x,0,z) = \begin{cases} V, & x_1 < x < x_2 \wedge z_1 < z < z_2, \\ 0, & \text{otherwise}. \end{cases} \tag{19}$$

The coefficients A_i are determined by taking the Fourier transform of this function, for example,

$$\begin{aligned} A_1(k_x,k_z) &= \frac{1}{\pi^2}\int_{-\infty}^{\infty} dz \int_{-\infty}^{\infty} dx \phi(x,0,z)\cos(k_x x)\cos(k_z z) \\ &= \frac{1}{\pi^2}\int_{z_1}^{z_2} dz \int_{x_1}^{x_2} dx V \cos(k_x x)\cos(k_z z) \\ &= \frac{V}{\pi^2 k_x k_z}[\sin(k_x x_2) - \sin(k_x x_1)] \\ &\quad \times [\sin(k_z z_2) - \sin(k_z z_1)], \end{aligned} \tag{20}$$

and similarly for the other A_i. Substituting these results into Eq. (18) and using trigonometric identities to simplify gives

$$\begin{aligned}\phi(x,y,z) = \frac{V}{\pi^2}\int_0^\infty dk_z \int_0^\infty dk_x \frac{e^{-\sqrt{k_x^2+k_z^2}y}}{k_x k_z}&\{\sin[k_x(x_2 - x)] \\ &- \sin[k_x(x_1 - x)]\}\{\sin[k_z(z_2 - z)] \\ &- \sin[k_z(z_1 - z)]\}.\end{aligned} \tag{21}$$

The integrals in this expression can be reduced by first taking a derivative with respect to x, finding the resulting integrals in standard tables [19], and reintegrating with respect to x. In general this procedure may introduce an integration constant that does not depend on x, but when the results are verified against the boundary conditions it is seen that no such integration constant is needed. The solution for the rectangular electrode boundary condition is

$$\phi(x,y,z) = \frac{V}{2\pi}\left\{ \arctan\left[\frac{(x_2-x)(z_2-z)}{y\sqrt{y^2+(x_2-x)^2+(z_2-z)^2}} \right] - \arctan\left[\frac{(x_1-x)(z_2-z)}{y\sqrt{y^2+(x_1-x)^2+(z_2-z)^2}} \right] - \arctan\left[\frac{(x_2-x)(z_1-z)}{y\sqrt{y^2+(x_2-x)^2+(z_1-z)^2}} \right] + \arctan\left[\frac{(x_1-x)(z_1-z)}{y\sqrt{y^2+(x_1-x)^2+(z_1-z)^2}} \right] \right\}. \quad (22)$$

Using this expression for the potential field of a single electrode, the field of an arbitrary set of rectangular electrodes can be constructed by summing together the fields of the individual electrodes.

It is possible to apply this same procedure to non-rectangular electrodes, although a closed-form expression for the field so far has been found only in the rectangular case. Evaluating these integrals numerically for non-rectangular electrodes may give results superior to finite-element field calculations.

In a linear Paul trap the rf electrodes are very long in the z dimension, so to analyze them it is useful to get an expression for the potential field in two dimensions by letting $z_1 \to -\infty$ and $z_2 \to \infty$:

$$\phi(x,y) = \frac{V}{\pi}\left[\arctan\left(\frac{x_2-x}{y}\right) - \arctan\left(\frac{x_1-x}{y}\right) \right]. \quad (23)$$

IV. rf ELECTRODE DESIGN

The model developed in the previous section can now be applied to the problem of designing a field which confines ions above the electrode surface. Some of the results of this section were developed independently and previously by Reichle *et al.*, but not published [20]. The electrodes that produce the rf field in the trap must be configured to create a local minimum in the absolute value of the rf electric field above the electrode surface. The location of this minimum is the trap center; it is the point about which a trapped ion will oscillate. Experiments typically use a combination of two rf electrodes with two or more electrodes held at rf ground to accomplish this, as shown in Fig. 1. Consider two rf electrodes that are infinitely long in the z dimension; one has edges at $x=-c$ and $x=0$, the other has edges at $x=a$ and $x=a+b$. The voltages applied to the electrode surface $y=0$ are

$$\phi(x,0,t) = \begin{cases} 0, & x < -c, \\ V_{\mathrm{rf}}\cos(\Omega t), & -c < x < 0, \\ 0, & 0 < x < a, \\ V_{\mathrm{rf}}\cos(\Omega t), & a < x < a+b, \\ 0, & x > a+b. \end{cases} \quad (24)$$

Here V_{rf} is the peak voltage applied to the rf electrodes and Ω is the rf angular frequency. The parameters a, b, and c describe the dimensions of the electrodes on the surface. This electrode configuration generalizes both the "five wire" and "four wire" geometries described by Chiaverini *et al.* [3], as discussed below. From Eq. (23), this configuration has the potential field

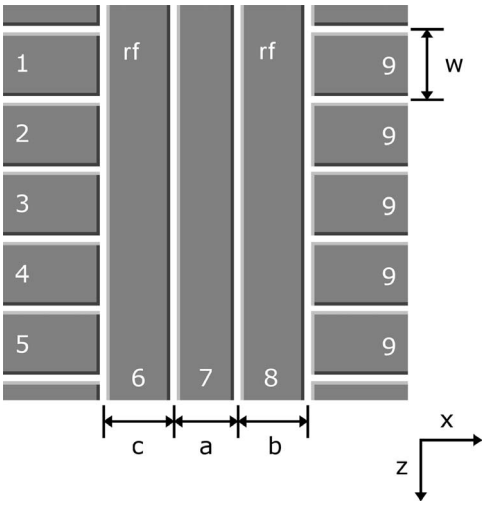

FIG. 1. Configuration of surface electrodes in the xz plane. The two segments marked "rf" are the rf electrodes; they are separated by a central electrode that is rf grounded. Outside of the rf electrodes are many independent control electrodes that are segmented in the z dimension in order to provide control over the ion's position in the z dimension. The parameters a, b, c, and w define the dimensions of the trap electrodes. The rf and central electrodes are assumed to extend infinitely in the z dimension, while the control electrodes are semi-infinite in x. Static voltages are applied to each electrode as numbered (see text).

$$\phi(x,y,t) = \frac{V_{\mathrm{rf}}}{\pi}\left[\arctan\left(\frac{a+b-x}{y}\right) - \arctan\left(\frac{a-x}{y}\right) - \arctan\left(\frac{x}{y}\right) + \arctan\left(\frac{c+x}{y}\right) \right]\cos(\Omega t). \quad (25)$$

In the xy plane the ion will be trapped around a point where the absolute value of the peak rf electric field is a local minimum. The electric field derived from Eq. (25) has a zero (necessarily a local minimum) above the electrode plane where the ion will be trapped, located at

$$x_0 = \frac{ac}{b+c}, \quad y_0 = \frac{\sqrt{abc(a+b+c)}}{b+c}. \quad (26)$$

The matrix Q defined by Eq. (5) can be determined explicitly by evaluating the second derivatives of the field at the center point, which gives

$$Q_{11} = -Q_{22} = \frac{-4ZeV_{\mathrm{rf}}}{\pi m\Omega^2}\frac{a^2(b^2-6bc+c^2)+a(b+c)(b^2-6bc+c^2)-bc(b+c)^2}{(a+b)^2(a+c)^2\sqrt{abc(a+b+c)}},$$

$$Q_{12} = Q_{21} = \frac{8ZeV_{\mathrm{rf}}}{\pi m\Omega^2}\frac{(b-c)(2a+b+c)}{(a+b)^2(a+c)^2}. \tag{27}$$

All other elements of Q are zero.

The pseudopotential has a saddle point above the trap center that represents the lowest potential that connects the local minimum region near the trap center with the region where the pseudopotential goes to zero as $y\to\infty$, which is the easiest point for an ion trapped inside the pseudopotential well to escape from the trap (see Fig. 2). The pseudopotential at this "escape point" represents the best estimate of the depth of the trap, i.e., the maximum energy at which an ion can be contained by the trap. An analytic solution for the location of this saddle point was not found except in a couple of specific cases discussed below. In general, the escape point can be found by solving numerically for the point above the trap center at which the gradient of the pseudopotential is zero. The pseudopotential at the escape point will usually be an upper bound on the actual trap depth since we must also consider the effect of the static field, which will most likely have negative curvature in the y direction under normal operating conditions, although a positive dc bias can be applied to the electrode plane while loading ions in order to increase the effective trapping potential until the ions can be cooled [10].

One trap design that has been experimented with, the "five wire" configuration, has rf electrodes as described in Eq. (24), with the two rf electrodes being of equal width so that $c=b$. For this configuration, the trap center is at $x_0=a/2$, $y_0=\sqrt{2ab+a^2}/2$. The escape point of the trap can be determined to be located at $x_E=a/2$, $y_E=\sqrt{2ab+a^2+2(a+b)\sqrt{2ab+a^2}}/2$. The trap depth is the pseudopotential at this point:

$$\psi_E = \frac{Z^2e^2V_{\mathrm{rf}}^2}{\pi^2m\Omega^2}\left[\frac{b}{(a+b)^2+(a+b)\sqrt{2ab+a^2}}\right]^2. \tag{28}$$

For a given value of a, ψ_E has a maximum at $b/a=\sqrt[3]{54-6\sqrt{33}}/6+\sqrt[3]{54+6\sqrt{33}}/6\approx 1.19149$. Thus by choosing the appropriate ratio of electrode sizes the trap design can be optimized to maximize the trap depth. The trapping potential is weaker if the rf electrodes are chosen to be too narrow or too wide relative to the center electrode.

Another design for the rf electrodes, called the "four wire" geometry, has one very wide outer rf electrode, with the other rf electrode equal in width to the center ground electrode. The result (25) applies, with the dimensions $c=a$ and $b\to\infty$. The center point of this trap is at $x_0=0$, $y_0=a$. The escape point is at $x_E=0$, $y_E=a\sqrt{2+\sqrt{5}}$, and the trap depth is

$$\psi_E = \frac{Z^2e^2V_{\mathrm{rf}}^2}{2(11+5\sqrt{5})\pi^2m\Omega^2a^2}. \tag{29}$$

If the center electrodes in the four wire geometry are asymmetric, $a\neq c$, the trap depth is less than it would be if both dimensions were equal to the smaller value.

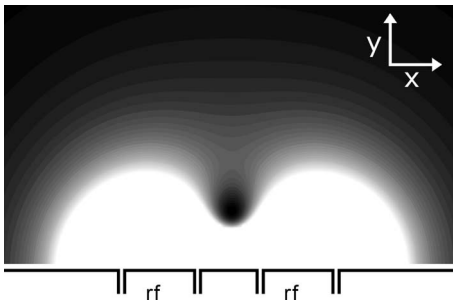

FIG. 2. Illustration of the pseudopotential well created by the electric fields of the surface electrodes, with the electrodes diagrammed at bottom. Dark shades correspond to low pseudopotential energy. The ion is to be trapped in the potential well near the center of the figure. The lowest energy path for the ion to escape the trap is through the saddle point in the pseudopotential directly above; the difference in pseudopotential between the center of the well and this escape point represents the maximum energy the ion can have and remain trapped. The top surface of the electrodes represent the $y=0$ plane. The electrodes labeled "rf" have the oscillating voltage applied to them; the others are rf grounded.

V. CONTROL ELECTRODE DESIGN

In the linear Paul trap the rf field provides trapping in the x and y dimensions; in the z dimension the ion is contained by a static potential. For surface electrode traps this can be achieved by segmenting the outer rf grounded electrode(s), as shown in Fig. 1, so that a static potential that is trapping in z can be produced by applying alternating voltages. The location of the trap center can be moved in z by varying the voltages applied to the control electrodes so that the minimum of the ion's potential well can be moved along the z dimension of the trap in a controlled way [21]. In order to avoid heating the ion as it is transported, it is desirable to maintain a constant value of the curvature of the potential in the z dimension, which is proportional to the matrix element A_{zz}. The width of a control electrode w should be chosen so that the field it creates has significant curvature everywhere along the path of the ion near the electrode. Figure 3 shows the potential curvature in z for an example case using the five wire geometry with $a=1$, $b=1.2$, and three different choices

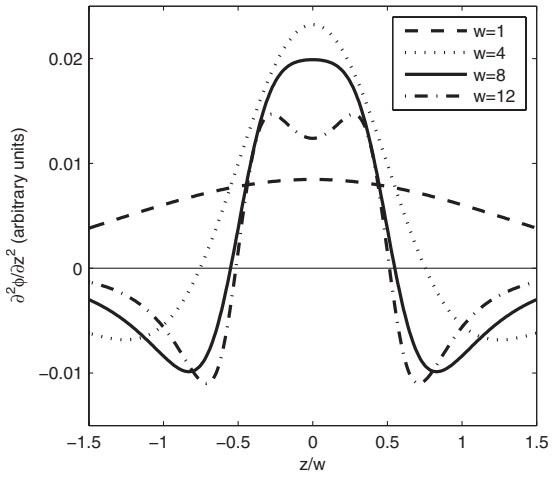

FIG. 3. Potential curvature in the z dimension at the trap center as a function of z/w for a single electrode segment with a 1 V applied voltage. $z=0$ is aligned with the center of the segment. The five wire configuration was used with parameters $a=1$, $b=1.2$. For small w, the curvature is relatively small. For large w, the curvature is reduced near the center of the segment, and a zero in the curvature approaches $z/w=\pm 0.5$ as w becomes larger. The neighboring segments, centered at $z=\pm w$, will therefore have a zero near the same point which means that the two nearest electrodes cannot contribute much to the curvature experienced by the ion at that point without applying large voltages to them.

for w. When w is relatively small, the potential at the trap center is small and the electrode's influence is relatively weak. If w is chosen very large, the potential tends to "flatten out" near the center of the electrode in z, and the potential curvature there is reduced. Of larger concern is the location of the zero of the potential curvature. As w increases, a zero in the potential curvature approaches $z=\pm w/2$, the edge of the electrode. This is an inconvenient place for it, since the neighboring electrode will also have a zero near the same edge. If the ion is to be shuttled across this point while maintaining the same value of A_{zz}, large voltages may be needed since no electrode can contribute strongly to the potential curvature at that point. This is likely the explanation for the instability predicted by Reichle *et al.* [21] for large control electrode widths, although the width recommended here is larger than their recommendation because the present potential model is three-dimensional instead of two-dimensional. For $b/a=1.2$ a good choice for the width is $w\approx 4a$.

An important task in trap design is to compute the electrode voltages required to trap an ion at location (x_0, y_0, z_0) while specifying the axial trap strength A_{zz}. The static electric field at the trap center of the rf field should be zero, otherwise an undesirable micromotion is produced [22]. Thus there are at least four constraints to consider when designing the static field: one to specify the curvature of the potential well in z, and three to nullify the electric field at the desired center point. In principle it takes at least four independent electrodes to generate such a field; in practice more are useful for a more robust field without excessive applied voltages. The set of voltages can be chosen to minimize the sum of the squares of the voltages

$$\text{minimize: } \sum_i V_i^2,$$

$$\text{subject to } \sum_i V_i \nabla \phi_i = \mathbf{0},$$

$$\sum_i V_i \frac{\partial^2 \phi_i}{\partial z^2} = \frac{m\Omega^2}{4Ze} A_{zz}, \tag{30}$$

where ϕ_i is the potential field of an individual electrode with unit voltage applied, V_i are the applied voltages, and all the fields are evaluated at the trap center. With the problem stated this way the voltages can be found using the method of Lagrange multipliers, which reduces to solving a system of linear equations in the unknowns V_i.

To illustrate the design considerations for the control electrodes, consider the following example trap design. The ion to be trapped is a singly ionized strontium atom, $Z=1$, $m=1.46\times 10^{-25}$ kg. The symmetric five-wire geometry is used with dimensions $a=100$ μm, $b=120$ μm. The rf field is generated by applying $V_{\text{rf}}=300$ V at frequency $\Omega=2\pi\times 50$ MHz. dc control voltages are applied to the electrodes as labeled in Figure 1; for example, voltage V_1 is applied to electrode 1. V_6 and V_8 are dc offsets applied to the rf electrodes. The control voltages can be applied symmetrically on each side, a symmetry which will lead to the ion equations of motions being uncoupled. To illustrate the coupling of the equations and that the control voltages do not need to be symmetric in x, for this example the entire right side of the electrode surface $x>a+b$ is tied together electrically and held at voltage V_9. For these parameters, the center of the trap is located at $x_0=50$ μm, $y_0=92.2$ μm. The escape point is at $x_E=50$ μm, $y_E=170$ μm, and the pseudopotential at the escape point is $\psi_E=0.184$ eV (although this trap depth is much less than a traditional Paul trap, it still can contain an ion at a temperature of roughly 2000 K). Initially the ion will be trapped at z position corresponding to the center of electrode 3 (chosen as $z=0$), with the axial stability parameter $A_{zz}=10^{-4}$. After finding the control voltages necessary to achieve these choices, the principal trap axes $\boldsymbol{b}_0$ are found to be in directions (0.668, 0.744, 0), (−0.744, 0.668, 0), and (0, 0, 1), with secular frequencies 11.5, 11.5, and 0.250 MHz, respectively. The control voltages can then be varied to move the ion along the z dimension. The voltages required to do so are shown in Fig. 4.

VI. CONCLUSION

The surface electrode type of ion trap appears to have a promising future due to the relative ease of constructing complex traps with very small dimensions, and the increased optical access they provide. This article has provided a discussion of the motion of an ion in such a trap as described by the coupled Mathieu equations, and an analytic model for determining the fields of the trap.

The coupling of the Mathieu equations does not seem to pose a significant problem for the experimenter. The qualitative behavior of the ion in the trap is the same; it is charac-

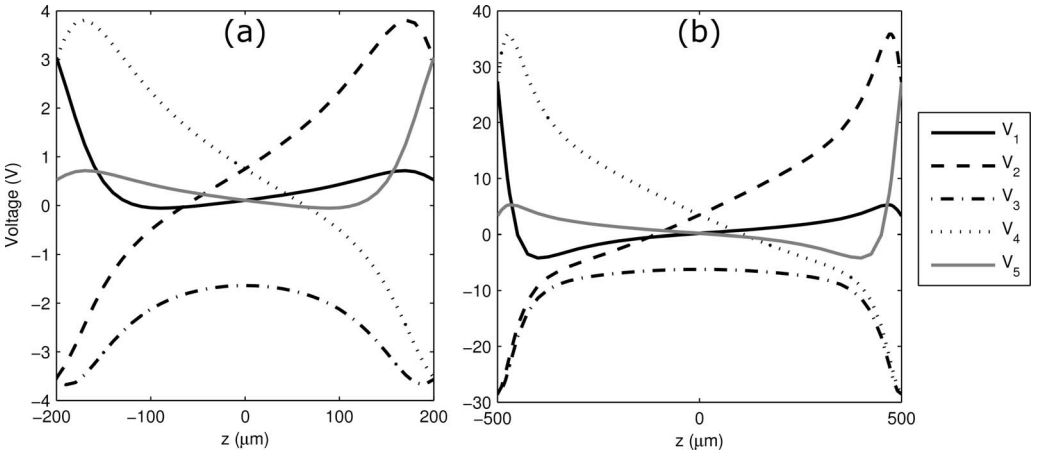

FIG. 4. Voltages applied to control electrodes in order to move an ion along the axial dimension of the trap while maintaining a constant A_{zz}. The trap parameters used are described in the text. Voltages are show for two control electrode widths: (a) $w=400$ μm, (b) $w=1000$ μm. The $z=0$ position corresponds to the center of electrode 3, and the z scale ranges from one edge of electrode 3 to the next. If the ion is moved past the edge of electrode 3 the roles of the electrodes can be switched so that the adjacent electrode is now electrode 3. Voltages 6–9, not shown for clarity, are small and nearly constant in both cases except near the edges of electrode 3. In the $w=1000$ μm case much larger voltages are required to achieve the same axial trap curvature A_{zz}, especially near the edges of the control electrodes.

terized by a fast micromotion and a slow secular motion. There are still three independent ion motional modes, but motion in each mode is not necessarily along one specific axis as it is when the equations decouple. Determination of the secular frequencies of the modes and the directions of the secular motion modes is more complicated but not different, in principle. This article has focused only on the classical motion of a single ion and not attempted to discuss the effect of the coupling of the fields when multiple ions are present, or on the quantum-mechanical description of an ion in the trap. It is expected that these will not change significantly from the one-dimensional motion description.

The solution of the Laplace equation (22) presented here is very general and may be useful for several applications. The focus here has been on surface electrode Paul traps, particularly the linear Paul trap, but the model could be adapted to study other types of Paul trap, or for other applications of the Laplace equation in electrostatics, elastostatics, and thermal conduction. One such application is dielectrophoresis, which also employs planar arrays of electrodes and for which similar analytic approaches have been developed [23–26].

The model given here can be arrived at by a mathematically equivalent approach which is to equate the electric field generated by an electrode with the magnetic field generated by a fictitious current flowing around the edge of an electrode. Such an approach arrives at the same solution for the field generated by the electrode; it may be a useful point of view for determining, either analytically or numerically, the fields of nonrectangular electrodes or relaxing other model assumptions.

The formulas developed here for trap parameters in terms of electrode geometry should make design of such traps easier and have been used to suggest optimizing the relative dimensions of the trap. They do not appear to favor either the four wire or five wire configuration; for similar dimensions both have similar trap characteristics. There may be room for improvement in the layout of control electrodes, especially for specific ion manipulations not studied here such as moving an ion around a corner, through a "T" junction, or bringing ions together and separating them in the trap. For example, it has been suggested that to separate two ions initially in a single potential well into two potential wells, a potential well that is initially quartic rather than quadratic is ideal [27]. Although generation of such potentials is not studied here, the present model can be applied to these problems.

ACKNOWLEDGMENTS

The author would like to thank R. Reichle for his helpful discussion of this paper and E. Kirilov for introducing the author to this topic.

APPENDIX: ELECTRODE GAPS

Two major simplifications were made about the electrode geometry in developing this model: that the electrode surface is infinite, and that there are no gaps between electrodes. The best approach found for addressing the finite size of the electrode surface is to assume that the potential is strictly zero on the $y=0$ plane outside the boundaries of the electrode surface. Doing so improves agreement with numerical simulations in all cases studied. The assumption that that there are no gaps between electrodes can be partially addressed analytically. Physically there must be an insulating gap between conductors in order for one electrode to be held at a different potential than an adjacent electrode. To assess the effect of small gaps between electrodes on the trap parameters, we apply the condition that the potential on the electrode plane changes linearly in the space between electrodes. Physically this is not a true requirement, but it is true to first order in the size of the gap and so it is adequate for modeling a small gap. Applying the method of Sec. III to the two-dimensional

boundary condition $\phi(x,y=0)=\Delta V(x-x_1)/(x_2-x_1)$ for $x_1 \leqslant x \leqslant x_2$ and $\phi(x,0)=0$ otherwise, the field solution

$$\phi(x,y)=\frac{\Delta V}{\pi(x_1-x_2)}\left\{\frac{y}{2}\ln\left[\frac{(x-x_1)^2+y^2}{(x-x_2)^2+y^2}\right]+(x-x_1)\times\left[\arctan\left(\frac{x-x_2}{y}\right)-\arctan\left(\frac{x-x_1}{y}\right)\right]\right\} \quad \text{(A1)}$$

is found. This result along with Eq. (23) can be used to construct an expression for the field of the symmetric five wire rf electrode geometry, modified by having gaps between the electrodes of width g, where the electric potential changes linearly in the gap. For example, $\phi(x,0)=(V_{\mathrm{rf}}/g)(x-a+g/2)$ on $a-g/2<x<a+g/2$, and ϕ changes similarly at the other boundaries between electrodes. The dimensions a and b describe the widths of the electrodes as measured from the center of one gap to the center of the next. With the gaps described this way, all of the interesting trap parameters determined without gaps in Sec. IV are modified only to second order in g. The trap center point is at $x_0=a/2$, $y_0=\sqrt{2ab+a^2-g^2}/2$, and the escape point is at $x_E=a/2$, $y_E=\sqrt{2ab+a^2-g^2+\frac{1}{2}\sqrt{(2ab+a^2)[(a+b)^2-g^2]}}/2$. Explicit expressions for the trap depth ψ_E and all the elements of the stability parameter matrix Q (too long to reproduce conveniently here) are also independent of g to first order. These formulas suggest that the gaps have only small effects on the overall potential field near the trap center, even when the size of the gap g is comparable to a and b (although as g becomes comparable to a and b, the model requirement that the field changes strictly linearly in the gap is less and less physically valid). This analysis shows that in order to maximize the accuracy of the model, the electrode dimensions (i.e., a, b, c, and w) should be measured from the center of one gap to the center of another, not from the true edges of the metal electrodes.

[1] W. Paul, Rev. Mod. Phys. **62**, 531 (1990).
[2] P. K. Ghosh, *Ion Traps* (Oxford University Press, New York, 1995).
[3] J. Chiaverini, R. B. Blakestad, J. Britton, J. D. Jost, C. Langer, D. Leibfried, R. Ozeri, and D. J. Wineland, Quantum Inf. Comput. **5**, 419 (2005).
[4] D. Kielpinski, C. Monroe, and D. J. Wineland, Nature (London) **417**, 709 (2002).
[5] D. J. Wineland, C. Monroe, W. M. Itano, D. Leibfried, B. E. King, and D. M. Meekhof, J. Res. Natl. Inst. Stand. Technol. **103**, 259 (1998).
[6] D. Leibfried, E. Knill, C. Ospelkaus, and D. J. Wineland, Phys. Rev. A **76**, 032324 (2007).
[7] J. Britton *et al.*, e-print arXiv:quant-ph/0605170v1.
[8] S. Seidelin *et al.*, Phys. Rev. Lett. **96**, 253003 (2006).
[9] C. E. Pearson, D. R. Leibrandt, W. S. Bakr, W. J. Mallard, K. R. Brown, and I. L. Chuang, Phys. Rev. A **73**, 032307 (2006).
[10] M. Cetina, A. Grier, J. Campbell, I. Chuang, and V. Vuletic, e-print arXiv:physics/0702025v1.
[11] D. R. Leibrandt, R. J. Clark, J. Labaziewicz, P. Antohi, W. Bakr, K. R. Brown, and I. L. Chuang, Phys. Rev. A **76**, 055403 (2007).
[12] K. R. Brown, R. J. Clark, J. Labaziewicz, P. Richerme, D. R. Leibrandt, and I. L. Chuang, Phys. Rev. A **75**, 015401 (2007).
[13] C. S. Hsu, J. Appl. Mech. **28**, 551 (1961).
[14] D. Leibfried, R. Blatt, C. Monroe, and D. Wineland, Rev. Mod. Phys. **75**, 281 (2003).
[15] A. H. Nayfeh and D. T. Mook, *Nonlinear Oscillations* (Wiley, New York, 1979).
[16] L. Cesari, *Asymptotic Behavior and Stability Problems in Ordinary Differential Equations*, 3rd ed. (Springer-Verlag, Berlin, 1971).
[17] H. G. Dehmelt, *Radiofrequency Spectroscopy of Stored Ions I: Storage* (Academic Press, New York, 1967), pp. 53–72.
[18] J. D. Jackson, *Classical Electrodynamics*, 3rd ed. (Wiley, Hoboken, 1999).
[19] I. S. Gradshteyn and I. M. Ryzhik, *Table of Integrals, Series, and Products*, 6th ed. (Academic Press, San Diego, 2000).
[20] R. Reichle *et al.* (unpublished).
[21] R. Reichle, D. Leibfried, R. B. Blakestad, J. Britton, J. D. Jost, E. Knill, C. Langer, R. Ozeri, S. Seidelin, and D. J. Wineland, Fortschr. Phys. **54**, 666 (2006).
[22] D. J. Berkeland, J. D. Miller, J. C. Bergquist, W. M. Itano, and D. J. Wineland, J. Appl. Phys. **83**, 5025 (1998).
[23] X. Wang, X. Wang, F. F. Becker, and P. R. C. Gascoyne, J. Phys. D **29**, 1649 (1996).
[24] M. Garcia and D. Clague, J. Phys. D **33**, 1747 (2000).
[25] H. Morgan, A. G. Izquierdo, D. Bakewell, N. G. Green, and A. Ramos, J. Phys. D **34**, 1553 (2001).
[26] D. E. Chang, S. Loire, and I. Mezic, J. Phys. D **36**, 3073 (2003).
[27] J. P. Home and A. M. Steane, Quantum Inf. Comput. **6**, 289 (2003).